



HAL
open science

The nature of the Laplace resonance between the Galilean moons

Giacomo Lari, Melaine Saillenfest

► **To cite this version:**

Giacomo Lari, Melaine Saillenfest. The nature of the Laplace resonance between the Galilean moons. *Celestial Mechanics and Dynamical Astronomy*, 2024, 136 (3), pp.19. 10.1007/s10569-024-10191-6 . hal-04594123

HAL Id: hal-04594123

<https://hal.science/hal-04594123>

Submitted on 31 May 2024

HAL is a multi-disciplinary open access archive for the deposit and dissemination of scientific research documents, whether they are published or not. The documents may come from teaching and research institutions in France or abroad, or from public or private research centers.

L'archive ouverte pluridisciplinaire **HAL**, est destinée au dépôt et à la diffusion de documents scientifiques de niveau recherche, publiés ou non, émanant des établissements d'enseignement et de recherche français ou étrangers, des laboratoires publics ou privés.



The nature of the Laplace resonance between the Galilean moons

Giacomo Lari¹ · Melaine Saillenfest²

Received: 11 January 2024 / Revised: 29 February 2024 / Accepted: 4 April 2024
© The Author(s) 2024

Abstract

The Laplace resonance is a mean-motion resonance that involves the three inner Galilean moons of Jupiter. However, its true nature is in part unclear; in particular, different views can be found in the literature on whether the Laplace resonance is a pure three-body resonance or a mere superposition of two-body resonances. To settle this question, we conduct a thorough analysis of the many resonances involved, starting from the two-body 2:1 commensurabilities of the couples Io–Europa and Europa–Ganymede, and ending with the three-body 4:2:1 commensurability between the three moons. By artificially varying the parameters of the system and monitoring its fundamental frequencies, we cartography all resonances involved and their interactions. From the analysis of the individual 2:1 commensurabilities, we find that despite the oscillation of the resonant angles they are not genuine resonances, as the trajectory of the system in the phase space is not enclosed by separatrices. On the contrary, as suggested by previous works, we show that the only current true mean-motion resonance is the pure three-body resonance between all three satellites. Moreover, we find that the current values of the moons’ orbital elements make the Laplace resonance sufficiently separated from the individual two-body 2:1 resonances, preventing chaotic effects from appearing.

Keywords Satellites · Mean-motion resonances · Fundamental frequencies

1 Introduction

The Galilean satellites of Jupiter, which in order from the planet are Io (1), Europa (2), Ganymede (3) and Callisto (4), are in an orbital configuration which is unique in the solar system. Indeed, the three inner moons are locked in a mean-motion resonance (MMR) for which their mean motions are nearly integer multiples: $n_1 \approx 2n_2 \approx 4n_3$. The resonant chain is composed by a 2:1 commensurability between Io and Europa, and a 2:1 commensurability between Europa and Ganymede. For each of these commensurabilities, we have an oscillating angle: let be λ_i the mean longitude of the i th satellite and ϖ_i its longitude of pericenter, we

✉ Giacomo Lari
giacomo.lari@unipi.it

¹ Dipartimento di Matematica, Università di Pisa, Largo Bruno Pontecorvo 5, 56127 Pisa, Italy

² IMCCE, Observatoire de Paris, PSL Research University, CNRS, Sorbonne Université, Université de Lille, 75014 Paris, France

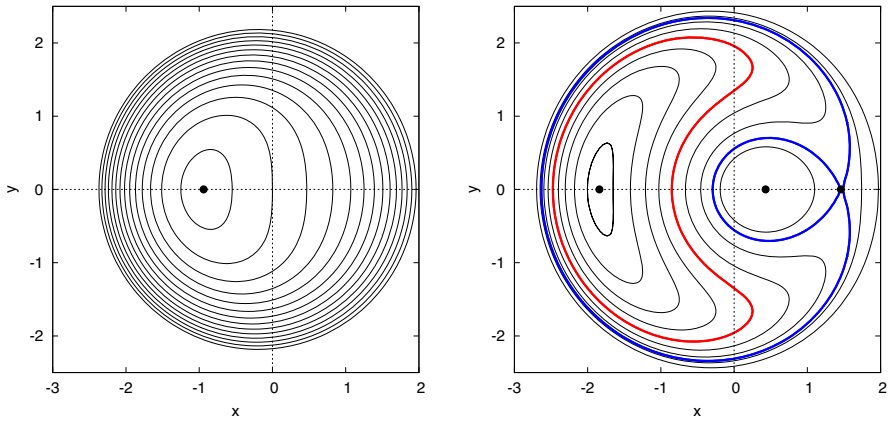


Fig. 1 Classic phase portraits of an integrable Hamiltonian for a first-order two-body MMR (Henrard and Lemaître 1983). On the left, the case with only one equilibrium point: all orbits circulate around the unique center point. On the right, the case with three equilibrium points: the phase space is divided in different regions by the separatrices (blue curves), which pass through the saddle point. The resonant region is the part of the space enclosed by the separatrices; an example of resonant curve is highlighted in red

currently have

$$\begin{aligned}
 \lambda_1 - 2\lambda_2 + \varpi_1 &\sim 0, \\
 \lambda_1 - 2\lambda_2 + \varpi_2 &\sim \pi, \\
 \lambda_2 - 2\lambda_3 + \varpi_2 &\sim 0,
 \end{aligned}
 \tag{1}$$

where symbol \sim stands for “closely oscillates around”. From the difference between the last two equations, we obtain:

$$\lambda_1 - 3\lambda_2 + 2\lambda_3 \sim \pi,
 \tag{2}$$

which involves the mean longitudes of all three satellites. This relation, or better the corresponding one between mean motions $n_1 - 3n_2 + 2n_3 \approx 0$, is commonly known as “Laplace resonance”.

By reviewing the past literature, we can note a persistent ambiguity on the nature of the Laplace resonance. Because of the many (two-body and three-body) resonant angles present in the system (see Eqs. 1, 2), it is not clear which commensurabilities correspond to actual resonances and different works often disagree about this. In particular, one could wonder whether the Laplace resonance is a superposition of two-body MMRs, so that Eq. (1) is just a geometric relation, or a genuine three-body resonance. This issue is pointed out for instance in the discussion at the end of Sinclair (1975), where Lieske argues that the oscillation of the two-body resonant angles observed by Sinclair has not the same dynamical meaning as the libration of the three-body resonant angle. Since then, several authors have referred to all current commensurabilities in the Galilean system as resonances (see, e.g., Yoder and Peale 1981; Malhotra 1991). In fact, Peale and Lee (2002) use the definition “Laplace relation” for the three-body commensurability, suggesting that the only genuine resonances are the two-body MMRs.

It is worth noting that the presence of an oscillating angle does not necessarily imply the establishment of a MMR. A resonance can be defined when the phase space features two qualitatively different families of trajectories delimited by a separatrix, as illustrated

in the right plot of Fig. 1. In this case, if we compute the fundamental frequencies of the system (Arnold 1989; Laskar 1993), we obtain a discontinuity between the orbits inside and outside the separatrix (e.g., Michtchenko et al. 2008). More precisely, when varying the parameters of a nearly integrable system, the crossing of a separatrix (and therefore the existence of a resonance) is revealed by the disappearance of one fundamental frequency, which is replaced by a new frequency, that we can relate to the libration of the resonant angle. When determining the fundamental frequencies of the Galilean system, Lainey et al. (2006) did not find fundamental frequencies associated with the 2:1 MMR of the couples Io–Europa and Europa–Ganymede, but only with the Laplace three-body resonance. Their conclusion was that the only genuine mean-motion resonance in the system is the three-body one between the three inner moons, even though the two-body angles in Eq. (1) are observed to oscillate. Gallardo et al. (2016) defines a three-body MMR as “pure” when it cannot be decomposed into a chain of two-body MMRs. In case the Laplace resonance is the only genuine MMR between the three moons, we can consider it to be pure.

While many analytical models have been developed to study two-body MMRs (see, e.g., Henrard and Lemaître 1983; Murray and Dermott 2000 and references therein), for three-body resonances the construction of such models is more challenging, as also second-order terms in the masses must be taken into account in the final averaged Hamiltonian (Nesvorný and Morbidelli 1998; Quillen 2011; Petit 2021). Apart from the Galilean moons, resonant chains and three-body MMRs are of much interest for exoplanetary systems (Luger et al. 2017; Siegel and Fabrycky 2021) and probably play or played a role in the evolution of other satellite systems (Quillen and French 2014; Ćuk and El Moutamid 2022). Gallardo et al. (2016) used a semi-analytical method to investigate the strength of three-body MMRs and applied it to their study of the Galilean satellites. They showed that the Laplace resonance affects the moons’ dynamics more than the individual 2:1 MMRs in terms of oscillations of semi-major axes and that it persists even under strong dissipative effects (see also Lari et al. 2020; Celletti et al. 2022). This apparent dominant role of the Laplace resonance suggests that the three-body MMR is indeed pure.

Most resonant models of the Galilean satellites found in the literature are based on an averaged Hamiltonian formulation which contains the 2:1 resonant terms of the mutual perturbations of the couples Io–Europa and Europa–Ganymede (see Sect. 2). The resulting dynamics includes the effects of the two-body resonances, but also the ones due to the emerging pure three-body resonance, so that when analyzing the moons’ motion it is not straightforward to determine which is the actual dominant resonance. Interpreting the Laplace resonance as a superposition of different two-body MMRs could be suggested by the behavior of the two-body resonant angles, but also by the forced values of the moons’ eccentricities, which can be obtained analytically from the individual two-body resonant terms of the Hamiltonian (Sinclair 1975). On the other hand, the results presented by Lainey et al. (2006) and Gallardo et al. (2016) lean toward a pure three-body MMR. Hence, the question is not settled, and good arguments in both directions can be found in the literature.

Several authors showed that it is possible to reduce the Laplace resonance dynamics in a pendulum-like motion (see, e.g., Yoder and Peale 1981; Henrard 1984; Showman and Malhotra 1997). This way, they built an analytical model with which it was possible to compute the libration frequency of the Laplace angle and the resonance width (see also Celletti et al. 2022). These results were obtained by forcing the two-body resonant angles to their equilibrium value and neglecting the moons’ free eccentricities. A recent work by Pucacco (2021) computed normal forms for the Laplace resonance in the vicinity of its equilibrium values, which allowed to obtain accurate analytical descriptions of the main dynamical features of the system (see also Henrard 1984). However, in order to compute

these normal forms, a given behavior must be assumed for the two-body angles, so that the dynamics can be averaged over fast variables. This implicitly assumes that the two-body commensurabilities are forced by the Laplace resonance; hence, in the approach followed by Pucacco (2021), the Laplace resonance is assumed a priori to be the only genuine resonance. Therefore, the most agnostic way of settling this question is to keep the Hamiltonian function to its lowest averaging level and to leave all commensurabilities free to vary over the course of numerical integrations.

In this context, our goal is to elucidate the nature of the Laplace resonance as we observe it today, with an eye on the possible pathways through which it has evolved toward its current state. To this aim, we build resonant models for the Galilean satellites and cartography the extent of the various (two-body and three-body) resonant regions through frequency analysis. A detailed study of the resonances at play provides a key information on the system and its past evolution. Indeed, it is still not sure whether the Laplace resonance was formed through subsequent resonant captures driven by tidal migration (on a billion-year timescale, see Yoder 1979; Yoder and Peale 1981) or directly into the circumjovian disk (on a million-year timescale, see Greenberg 1982; Peale and Lee 2002). Different orbital evolutions imply different histories for the resonances of the system (see also Tittlemore 1990; Showman and Malhotra 1997), whose final result is constrained by the current configuration of the moons.

The paper is structured as follows: in Sect. 2, we introduce the dynamical model we use for describing the motion of the moons and the process of frequency analysis we apply to the numerical integrations. In Sect. 3, we analyze the case of two-body resonances, focusing on the 2:1 commensurabilities of the couples Io–Europa and Europa–Ganymede, while, in Sect. 4, we analyze the Laplace resonance between the three moons. In Sect. 5, we discuss the current resonant state of the Galilean system and its possible evolution in light of the results presented in the previous sections. Finally, in Sect. 6, we summarize the obtained results.

2 Dynamical model

As we want to investigate the resonant dynamics of the system, we use an averaged model where we remove all short-period terms, which are unimportant for resonant and secular timescales. This way, the relevant frequencies will be easier to detect and identify by the frequency analysis (see below). Averaged models also allow large portions of the parameter space to be explored in reasonable computing time. As all current resonances in the system are eccentricity type, we consider a planar motion for the satellites, neglecting their small inclinations. This choice allows us to keep the model as simple as possible while still capturing the essence of the dynamics. For a more complete model of the averaged dynamics of the satellites, we refer to Lari (2018), which has been proven to reproduce well both the resonant and secular features of the Galilean system. On long timescales, tidal dissipation in the Jovian system produces a slow drift in the moons' orbits (Lari et al. 2020, 2023). However, here we are only interested in the current state of the moons, so we neglect tides and we keep only the main terms of the dynamics (see also Malhotra 1991).

Let be \mathcal{G} , m_0 , R_J and J_2 the gravitational constant, the mass, equatorial radius and quadrupole moment of Jupiter, respectively, while m_i and $\beta_i = m_0 m_i / (m_0 + m_i)$ ($i = 1, 2, 3$) are the Galilean satellites' masses and reduced masses. We neglect the gravitational effect of Callisto here ($i = 4$), as it is not currently involved in any resonance and its contribution to the resonant dynamics is unimportant. We describe the motion of the satellites through their Keplerian elements $(a_i, e_i, \varpi_i, \lambda_i)$, which are the semi-major axis, eccentricity, longi-

tude of the pericenter and mean longitude, respectively. We introduce also the mean motion $n_i = \sqrt{\mathcal{G}(m_0 + m_i)/a_i^3}$.

We use an equatorial frame centered at Jupiter and neglect the motion of its spin axis, so that our full averaged model is described by the Hamiltonian

$$\mathcal{H} = \mathcal{H}_0 + \varepsilon \mathcal{H}_1, \tag{3}$$

which is split in the Keplerian part

$$\mathcal{H}_0 = - \sum_{i=1}^3 \frac{\mathcal{G}m_0m_i}{2a_i}, \tag{4}$$

and the perturbation

$$\varepsilon \mathcal{H}_1 = \mathcal{H}_J + \mathcal{H}_M. \tag{5}$$

In the perturbative function, we consider the oblateness of Jupiter and the mutual gravitational attraction of the satellites. The expression of their corresponding Hamiltonian functions is

$$\mathcal{H}_J = \sum_{i=1}^3 \frac{\mathcal{G}m_0m_i}{a_i} \left[J_2 \left(\frac{R_J}{a_i} \right)^2 \left(-\frac{1}{2} - \frac{3}{4} e_i^2 \right) \right] \tag{6}$$

and

$$\mathcal{H}_M = \mathcal{H}_M^{(1\text{ord})} + \mathcal{H}_M^{(2\text{ord})} \tag{7}$$

that we split in first-order and second-order terms with respect to eccentricities. The first part is

$$\begin{aligned} \mathcal{H}_M^{(1\text{ord})} = \sum_{ij=(12,23)} \left[\frac{\beta_i n_i a_i \beta_j n_j a_j}{m_0} e_j \cos(2\lambda_j - \lambda_i - \varpi_j) \right. \\ \left. - \frac{\mathcal{G}m_i m_j}{a_j} \left(f_{27} e_i \cos(2\lambda_j - \lambda_i - \varpi_i) \right. \right. \\ \left. \left. + f_{31} e_j \cos(2\lambda_j - \lambda_i - \varpi_j) \right) \right], \tag{8} \end{aligned}$$

which contains only resonant terms, and the other part is

$$\begin{aligned} \mathcal{H}_M^{(2\text{ord})} = - \sum_{1 \leq i < j \leq 3} \frac{\mathcal{G}m_i m_j}{a_j} \left(f_1 + f_2(e_i^2 + e_j^2) + f_{10} e_i e_j \cos(\varpi_j - \varpi_i) \right) \\ - \sum_{ij=(12,23)} \frac{\mathcal{G}m_i m_j}{a_j} \left(f_{45} e_i^2 \cos(4\lambda_j - 2\lambda_i - 2\varpi_i) \right. \\ + f_{53} e_j^2 \cos(4\lambda_j - 2\lambda_i - 2\varpi_j) \\ \left. + f_{49} e_i e_j \cos(4\lambda_j - 2\lambda_i - \varpi_i - \varpi_j) \right), \tag{9} \end{aligned}$$

which contains both resonant and secular terms. We included the term f_1 in Eq. (9), even though its actual order is zero, as its contribution to the resonant dynamics is minor (it contributes almost as a constant term in the Hamiltonian function). The first term in Eq. (8), which comes from the indirect part of the perturbation, can be included in the third one just

Table 1 Mean semi-major axes and eccentricities of Io, Europa, and Ganymede at J2000 epoch. Values of semi-major axes are given in Jupiter's radii ($R_J = 71398$ km)

	Io	Europa	<i>Ganymede</i>
a	5.9191	9.4147	15.0157
e	0.0041	0.0095	0.0015

changing the definition of f_{31} . The above Hamiltonian functions are already averaged and truncated at the second order in eccentricities. The coefficients f_k in Eqs. (8) and (9) are combinations of Laplace coefficients and depend on the ratio of the semi-major axes a_i/a_j . Their expression can be found in Murray and Dermott (2000). We note that, if in Eq. (7) we neglect second-order terms, the Hamiltonian function only contains the two resonant terms with arguments $(2\lambda_j - \lambda_i - \varpi_i)$ and $(2\lambda_j - \lambda_i - \varpi_j)$.

From the Hamiltonian in Eq. (3), written in suitable canonical coordinates (see, e.g., Lari 2018), we can compute the equations of motion. In this work, we consider the following canonical angle coordinates: $-\varpi_i$ ($i = 1, 2, 3$) and $\lambda_i - 2\lambda_{i+1}$ ($i = 1, 2$), so that the final system results to have five degrees of freedom. Actually, it is possible to use a more efficient canonical transformation which removes a further degree of freedom (Henrard 1984; Malhotra 1991; Pucacco 2021). However, we prefer to employ variables which are easily comparable to the case we remove or add a satellite in the model (Lari et al. 2020). The values of all parameters and moons' mean initial conditions at J2000 epoch can be found in Lari et al. (2020). For convenience, in Table 1 we reported only the values of semi-major axes and eccentricities.

In this article, our goal is to scan the phase space around the current location of the Galilean satellites in order to locate the various resonant regions. Therefore, we perform a frequency analysis over a grid of initial conditions, varying one parameter at a time, and we monitor the behavior of each fundamental frequency. In general, if we consider an integrable approximation of the system (and under some technical conditions), there exists a set of action-angle coordinates such that the actions are constant and the angles circulate with constant frequencies (see Arnold 1989). If the system is non-degenerate, there is a one-to-one relation between the actions and the constant fundamental frequencies. In a one-degree-of-freedom model as that illustrated in Fig. 1, the constant action is directly related to the area enclosed by the trajectory. We see that there is a qualitative difference in the definition of action variables for resonant and non-resonant trajectories, with a discontinuity occurring on the separatrix. This discontinuity is a characteristic of the presence of a resonance and is reflected in the computation of the fundamental frequencies of the system.

In practice, we perform hundreds of integrations of the moons' system, changing either the initial condition of the semi-major axis or the eccentricity of a single moon. For each integration, we set an integration time of 2000 years and a time step of 0.03 years. Using the software TRIP (Gastineau and Laskar 2011), we perform the spectral analysis of the time evolution of the system and we obtain numerically an estimate of its fundamental frequencies (Laskar 1988, 1993). Following the evolution of the fundamental frequencies when the parameters vary, we can identify the location of the different resonances and their possible interactions.

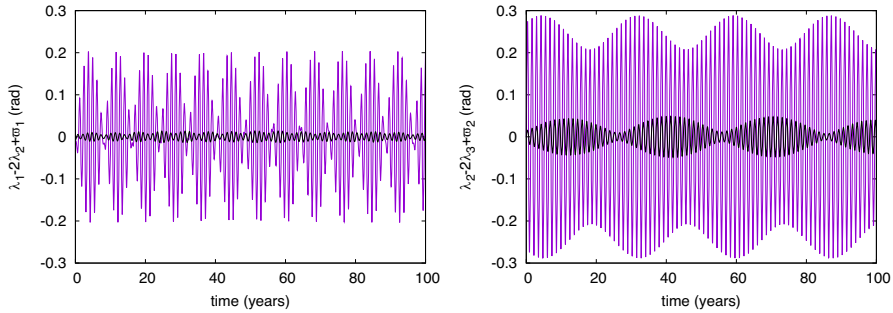


Fig. 2 Behavior of the two-body resonant angles of the 2:1 commensurabilities for the couples Io–Europa (left) and Europa–Ganymede (right). The violet curve is obtained integrating the system without the third moon, while the black with all three moons

3 Two-body resonances in the Galilean system

In this section, we investigate the current state of the 2:1 commensurabilities of the couples Io–Europa and Europa–Ganymede. We know that $n_1 - 2n_2 \approx 0$ and $n_2 - 2n_3 \approx 0$, but do these commensurabilities correspond to genuine two-body MMRs? A naive but simple way to answer to this question is to remove one of the satellites (Io or Ganymede), so that the three-body MMR vanishes and there is only one 2:1 commensurability. The motion of the two remaining moons can be described by the model presented in Sect. 2, considering the sums over two bodies, instead of three (i.e., removing the index 1 or 3). For simplicity, we use the same initial conditions, even though the removal of one of the satellites makes the mean orbital elements slightly change.

We stress that the system obtained here is artificial; it does not realistically reproduce the behavior of the real moons and it is not supposed to do so. The initial conditions are also not physically realistic because in reality the Galilean moons have relaxed for billions of years toward an equilibrium configuration composed of three resonant bodies instead of two. This simplified setting is used here on purpose as a tool to map the resonant regions.

From Fig. 2, we can see the behavior of the two-body resonant angles. Their oscillation amplitudes are quite small, even though they are higher when considering only two moons than when considering the complete system, as shown in the figure. As explained above, this is due to the fact that we took the same initial conditions even though the dynamical system is different. The fact that the angles oscillate in the two cases could suggest that these 2:1 commensurabilities are real resonances. However, as explained in Sect. 1, this condition is not sufficient, and we must verify whether the resonant orbit is enclosed between separatrices.

In order to investigate this point, we analyze the phase portrait of the simplified problem. Indeed, two-body 2:1 MMRs can be described by an integrable one-degree-of-freedom Hamiltonian, but it is necessary to perform some approximations of the dynamics. We use the classic approach and only keep first-order terms in the model, so that all secular terms of the mutual perturbation between the moons and the oblateness of the planet are neglected. Between the different formulations presented in the literature (starting from Henrard and Lemaître 1983), we use the model presented in Batygin and Morbidelli (2013), which differently from the restricted case (see, e.g., Murray and Dermott 2000), takes into account both first-order resonant terms present in Eq. (8). Such a model reduces the initial Hamiltonian

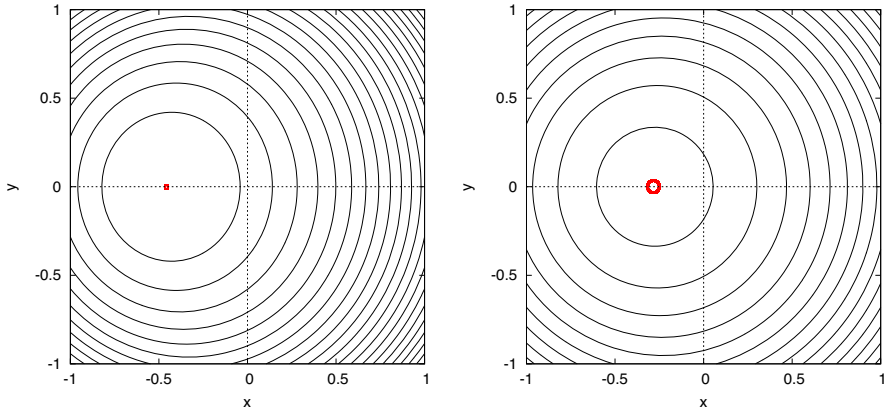


Fig. 3 Phase space of the 2:1 MMR for Io–Europa (left) and Europa–Ganymede (right). The black curves are the level curves of the integrable one-degree-of-freedom Hamiltonian, while the red curves are the orbits of the two systems considering their current mean orbital elements

(with only two satellites)

$$\mathcal{H} = \mathcal{H}_0 + \mathcal{H}_M^{(1\text{ord})} \tag{10}$$

to an integrable one-degree-of-freedom Hamiltonian defined as (see Eq. 29 of Batygin and Morbidelli 2013),

$$\tilde{\mathcal{H}} = \hat{\delta}(\Omega + \Psi_1 + \Psi_2) - (\Omega + \Psi_1 + \Psi_2)^2 - \sqrt{2\Psi_1} \cos \psi_1 \tag{11}$$

which is equivalent to the second fundamental model for (first-order) resonances (Henrard and Lemaître 1983). In Eq. (11), the only variables are the coordinate ψ_1 , which is a combination of the two resonant arguments, and its momentum Ψ_1 , which is related to the eccentricities of the bodies. All other quantities are constant, and their definition can be found in Batygin and Morbidelli (2013).

Considering the parameters and the initial conditions (in mean elements) of the Galilean system, for the couples Io–Europa and Europa–Ganymede, we obtain the phase portraits in Fig. 3. They are represented in the Cartesian plane (x, y) , where $x = \sqrt{2\Psi_1} \cos \psi_1$ and $y = \sqrt{2\Psi_1} \sin \psi_1$. As the orbits (red curves) do not surround the origin, the resonant angles indeed oscillate around a fixed value, as shown also in Fig. 2. However, the orbits correspond to a circulation around a center shifted from origin. Indeed, given the values of the parameters and the current moons’ orbits, both systems have only one stable equilibrium point, so that the saddle point and its separatrices do not appear in the phase portrait (compare with Fig. 1). Therefore, the orbits are not enclosed between separatrices and the moons are not locked in a true resonance.

However, despite this, the two-body resonant interaction between the moons has significant effects on the dynamics, as evidenced by the forced value of the moons’ eccentricities, which is due to the shift of the equilibrium point toward the left caused by the proximity to the two-body MMR. Indeed, the nonzero eccentricity of Io ($e_1 = 0.0041$, see Table 1) is almost entirely due to the two-body first-order term with argument $2\lambda_2 - \lambda_1 - \varpi_1$, which gives a proportional relation between $-\dot{\varpi}_1$ (that follows the commensurability) and $1/e_1$ (see, e.g., Yoder and Peale 1981). With the current value of $n_1 - 2n_2$, we obtain $e_1 \approx 0.0045$. Pucacco (2021) presented a more accurate estimate of the forced values of the moons’ eccentricities,

Table 2 Fundamental frequencies (rad/day) of the Io–Europa system, considering a dynamical system including first and second-order terms in eccentricities of the model presented in Sect. 2

a_1	g_1	g_2	ν
5.90	0.002389	0.000510	0.029704
5.92	0.002731	0.000548	0.011695
5.94	0.005633	0.001146	0.001264
5.96	0.002491	0.000551	-0.022006

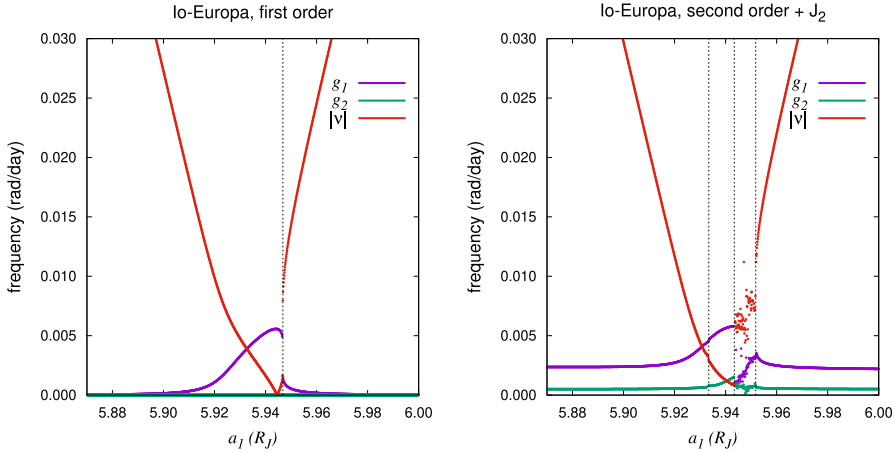


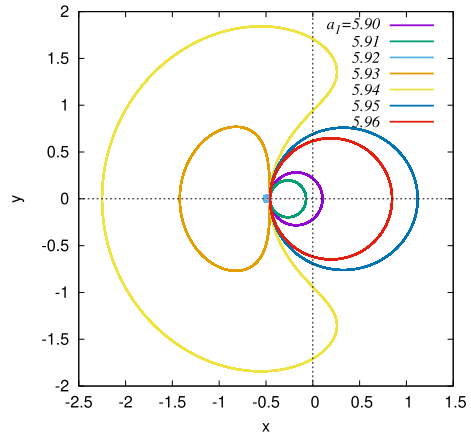
Fig. 4 Evolution of the fundamental frequencies for the Io–Europa system in function of the value of a_1 . We consider two different models: only first-order terms (left), also second-order and J_2 terms (right). Vertical asymptotes and chaotic regions reveal the encounter with a separatrix

which come from the analytical expression of the equilibrium points of the system with all three satellites. Just like Io, also Europa’s forced eccentricity is mainly the result of two-body interactions and an estimate can be obtained considering the dynamical effect of the first-order terms $2\lambda_2 - \lambda_1 - \varpi_2$ (Io’s perturbation) and $2\lambda_3 - \lambda_2 - \varpi_2$ (Ganymede’s perturbation). Differently from the first two satellites, Ganymede’s eccentricity has a significant free component (see, e.g., Sinclair 1975). Due to this strong effect of the nearby two-body resonances, one can easily be misled into thinking that these commensurabilities are genuine resonances and that they dominate the Galilean satellites’ dynamics.

The results obtained so far rely on a largely approximated model of the moons’ dynamics. In order to work with a more realistic model, we need to re-include most terms of the dynamical model presented in Sect. 2. In this way, however, we lose the one-degree-of-freedom expression of the Hamiltonian, and the phase space is not described anymore through simple two-dimensional curves. Nevertheless, we can analyze the fundamental frequencies of the system, in order to investigate its dynamical features. We follow the evolution of the fundamental frequencies while varying one of the system’s parameters, in order to see how they change from within to outside the MMR. We consider the resonant system composed by Io and Europa (the case of Europa and Ganymede is similar) and we show the results obtained by changing slightly the initial mean value of a_1 .

As in the averaged model we have three angle variables, there are three fundamental frequencies: g_1 , g_2 and ν (see Table 2). The frequencies g_1 and g_2 are associated with the secular precession of the pericenters ϖ_1 and ϖ_2 , respectively. The frequency ν is associated

Fig. 5 Orbits of the Io–Europa system in the one-degree-of-freedom phase space, considering different initial values of a_1



with the behavior of the combination of mean longitudes $\lambda_1 - 2\lambda_2$. Far from the resonance, the moons’ orbital motions are decoupled, such that $\nu \approx n_1 - 2n_2$. However, close to the resonance, the value of ν is dictated by the resonant dynamics, either in the case of libration or circulation. We note that the frequencies g_1, g_2 and ν are not always the dominant terms in the quasi-periodic approximation of the dynamics obtained through the frequency analysis. Therefore, the correct identification of each frequency requires to carefully follow their behavior from outside to inside the resonance.

In Fig. 4, we report the plot of the fundamental frequencies g_1, g_2 and ν . We considered two different levels of approximation of the dynamics. The left plot of Fig. 4 shows the frequencies for the simplest model (only first-order terms and neglecting the oblateness of Jupiter), which is almost equivalent to the integrable model defined by Eq. (11). If we read the plot from left to right, we can see how the frequency ν (red curve) starts from high values ($\nu > 0$, see Table 2), as the system is far from the resonance (the nominal 2:1 resonance is at $a_1 \approx 5.931 R_J$). As a_1 increases, ν decreases and the system approaches the resonance. The fundamental frequency evolves smoothly inside the resonance; in fact, there is no clear discontinuity which indicates the entrance into resonance, as the orbit does not cross the separatrices, but it remains trapped inside when they appear. However, from the integrable Hamiltonian approximation (see Fig. 5), we can compute the value of a_1 for which three equilibrium points appear, that results to be a bit smaller than $5.940 R_J$ (note that the current value is $a_1 = 5.919 R_J$, see Table 1). As we continue to increase the value of a_1 , finally the orbit encounters the separatrix and the frequency combination $\nu + g_1$ goes to 0. In the plot, we can see a vertical asymptote for the frequencies at around $a_1 \approx 5.947 R_J$; this is due to the separatrix crossing: the system passes instantaneously from a libration regime to a circulation regime. Moving further, if we take values of $a_1 > 5.947 R_J$, we see that the absolute value of the frequency increases rapidly (here $\nu < 0$, Table 2), as the system is again outside the resonance and moves away from it.

In Fig. 5, we can appreciate how the orbits change in the one-degree-of-freedom phase space for different values of a_1 , while we keep the same value for the other orbital elements. Only for $a_1 = 5.94 R_J$, which is in the interval $(5.940, 5.947) R_J$, we have a genuine resonant orbit, while the others represent circulating or librating orbits not enclosed within separatrices. All curves in Fig. 5 pass through a common point, because the initial conditions for eccentricities and resonant angles are the same for all considered orbits.

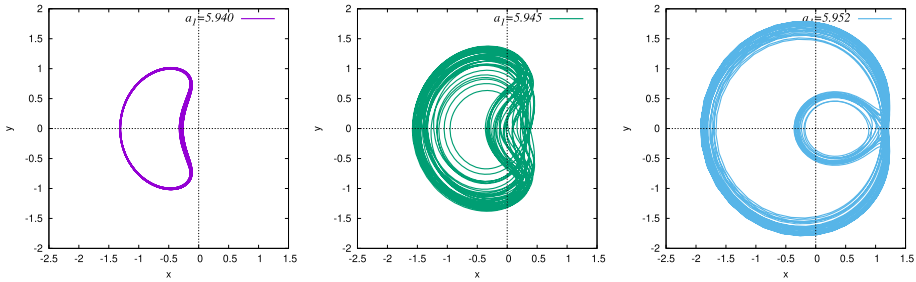


Fig. 6 Orbits of the Io–Europa system in the phase space (x, y) , considering three different initial values of a_1 . In this case, as we consider second-order terms in the Hamiltonian, the system is not integrable and the orbits do not follow precisely the curves defined by the resonant Hamiltonian

The other plot in Fig. 4 (right) shows again the evolution of the fundamental frequencies, but with a more complete model of the 2:1 resonant system, which includes J_2 and second-order terms of the mutual gravitational perturbation. The first difference we note with respect to the plot on the left is that the secular frequencies g_1 and g_2 starts from values significantly higher than in the previous case. This is due to the secular perturbations (previously neglected), which makes Io and Europa’s pericenters precess. In general, as $\dot{\omega}_1 > 0$, the resonance position $(n_1 - 2n_2 + \dot{\omega}_1 = 0)$ results to be slightly shifted toward right (in terms of a_1 values) with respect to its nominal location $(n_1 - 2n_2 = 0)$.

The evolution of the frequency ν outside the resonance is very similar to the one already described. Interestingly, at $a_1 \approx 5.933 R_J$, we can note a small discontinuity of the fundamental frequencies, which is due to the crossing of a secondary resonance given by the combination $\nu + g_2 - (g_1 - g_2) = 0$. However, we find a completely new behavior of the frequencies once the system enters the resonance region. Indeed, we can observe that, from $a_1 \approx 5.943 R_J$, the fundamental frequencies start to show chaotic effects, which persist up to $\approx 5.952 R_J$. If we plot the orbits in the plane (x, y) , we see a major difference with the case of the integrable system: in that case, the orbits moved on the fixed level curves of the Hamiltonian (see Fig. 5), while now the orbits can vary greatly, exploring a whole range of curves of the space (see Fig. 6). This is due to the non-integrable nature of the system; nevertheless, we can find orbits that present just small deviations from the level curves, while for other we have extremely wide variations. This difference is due to the orbits’ distance from the separatrices. Indeed, if a considered orbit is close enough to the separatrices, the perturbation to the resonant motion can push the orbit to cross them. The orbit can then jump through different regions of the phase space, which make its path chaotic. In the right plot of Fig. 6, we can recognize the shape of the separatrix of the MMR and how the orbit moves between its outer and inner regions. Instead, for orbits far from separatrices or in the case they are not present, the motion follows approximately close curves (left plot).

Although on one hand the chaos adds complexity to the description of the dynamics, on the other it helps to recognize the location of the resonance in the case of a non-integrable system. Indeed, the chaos indicates the presence of separatrices, therefore of the resonance.

In the end, thanks to the analysis of the fundamental frequencies, we have a general view of the various regions of the 2:1 MMR, which will be useful to interpret some of the results on the complete model with all three satellites.

Table 3 Fundamental frequencies (rad/day) of the Io–Europa–Ganymede system, considering a dynamical system including first and second-order terms in eccentricities of the model presented in Sect. 2

a_1	g_1	g_2	g_3	ν_1	ν_2	μ
5.90	0.002475	0.000787	0.000131	0.029492	0.013102	–
5.92	0.002705	0.000672	0.000132	0.012616	–	0.003091
5.94	*	*	*	*	*	*
5.96	0.002582	0.000860	0.000132	–0.021953	0.012182	–

For $a_1 = 5.94 R_J$ we did not report any value (symbol '*'), as the motion is affected by chaos, so that it cannot be approximated by quasi-periodic series. Symbol '-' means that the corresponding frequency is not present or is not an independent fundamental frequency of the system

4 Mapping the Laplace resonance

In this section, we consider the system with all three satellites. In particular, we want to analyze the Laplace resonance and find evidences that it is a pure three-body MMR, i.e., not just the geometric consequence of a chain of two two-body MMRs. We aim also at determining how the emergence of the Laplace resonance relates with the 2:1 two-body resonances we studied in the previous section.

As in our dynamical model we have five angle variables, there are five fundamental frequencies: the three secular frequencies g_1 , g_2 and g_3 associated with the precession of the pericenters, and other two frequencies associated with the combinations of mean longitudes (see Table 3). Outside all resonances, we can consider the two separate frequencies ν_1 and ν_2 associated with the circulation of $\lambda_1 - 2\lambda_2$ and $\lambda_2 - 2\lambda_3$, respectively. However, inside the resonant region, the values of ν_1 and ν_2 are dictated by the resonant dynamics. In particular, we are interested in their behavior when the Laplace resonance is active.

In Fig. 7, we show two plots similar to the ones already presented in Sect. 3. On the left, we have the case of the model with only first-order terms of the mutual perturbations between the three moons, while on the right the model includes also the second-order terms presented in Sect. 2. Apart from the values of the secular fundamental frequencies, which differ in the two setups because of the secular perturbations, the two plots are very similar. Therefore, in our analysis, we will focus on the results for the more complete model.

As we change only a_1 and we take the other initial conditions equal to their actual values, the 2:1 commensurability between Europa and Ganymede is preserved, while we move Io in order to explore the other resonances. This is reflected in the values of the frequencies ν_1 and ν_2 : the frequency ν_1 decreases fast on the left ($\nu_1 > 0$) and right ($\nu_1 < 0$) of the resonant region, while ν_2 remains almost constant. Interestingly, at $a_1 \approx 5.903 R_J$, we can note a small discontinuity in the fundamental frequencies, which is due to the crossing of a secondary resonance close to the combination $\nu_1 - 2\nu_2 \approx 0$.

Moving on the right of the plot, we encounter a major change of the system at $a_1 = 5.911 R_J$, due to the activation of the three-body resonance. The frequencies ν_1 and ν_2 become equal such that the system loses one fundamental frequency (the yellow and red line coincide in the plot), and a new fundamental frequency μ appear (orange line). This is the fundamental frequency associated with the libration of the three-body resonant angle $\lambda_1 - 3\lambda_2 + 2\lambda_3$, and we manage to identify it for $a_1 \in (5.911, 5.930) R_J$. In this interval, the system is described by the fundamental frequencies (ν_1, μ) instead of (ν_1, ν_2) (see Table 3). Indeed, the individual frequencies ν_1 and ν_2 disappear, and are replaced by a single fundamental frequency. We can retrieve this frequency either from the analysis of the time series of $\lambda_1 - 2\lambda_2$ or $\lambda_2 - 2\lambda_3$. To

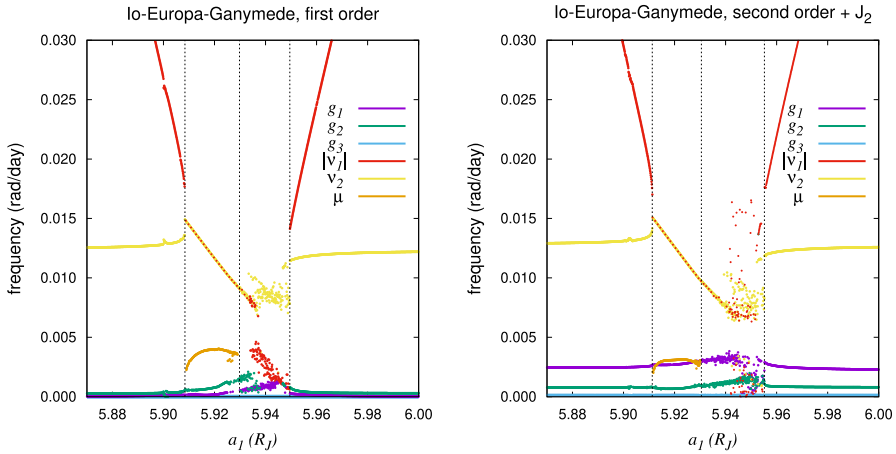


Fig. 7 Evolution of the fundamental frequencies for the Io–Europa–Ganymede system in function of the value of a_1 . We consider two different models: only first-order terms (left), also second-order and J_2 terms. Vertical asymptotes and chaotic regions reveal the encounter with a separatrix

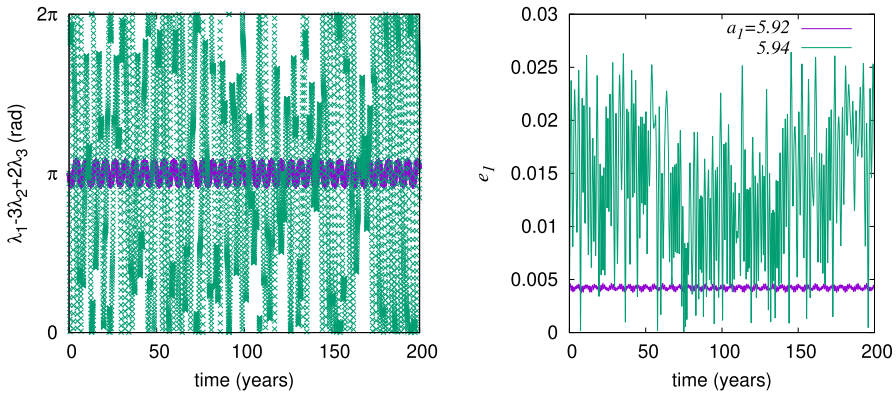


Fig. 8 Evolution of the Laplace resonance angle and the eccentricity of Io considering two propagations, one with $a_1 = 5.92 R_J$ (violet) and the other $a_1 = 5.94 R_J$ (green) as initial condition

emphasize this fact, in Fig. 7, we have plotted both the yellow line (coming from the analysis of $\lambda_2 - 2\lambda_3$) and superimposed red dots (coming from the analysis of $\lambda_1 - 2\lambda_2$). As the current value of a_1 is inside this range ($a_1 = 5.919 R_J$, see Table 1) and we know that the individual two-body resonances are not enclosed by separatrices, we can state that the system is in a pure three-body MMR (see also Lainey et al. 2006). If we observe the evolution of the frequency μ , we can see that it is similar to an inverted U, so that its values are smaller at the extremes of the interval, while it has a maximum close to the center. This behavior suggests that both at left and right we are approaching a separatrix of the three-body resonance, and that today we are close to the center of the resonance. This relaxed configuration of the system is probably the result of tidal dissipation over hundred million years (Yoder and Peale 1981). It is worth noting that, inside the three-body resonance, the frequency ν_1 (or ν_2) is forced to decrease almost linearly. This behavior allows to maintain the three-body relation $n_1 - 3n_2 + 2n_3 \approx 0$ as we continue to increase a_1 .

Table 4 Frequency analysis and identification for the system including Io, Europa and Ganymede, and taking $a_1 = 5.92 R_J$ as initial condition (which is very close but not equal to the actual value)

Series	Frequency (rad/day)	Amplitude	g_1	g_2	g_3	ν_1	μ
$a_1 (R_J)$	0.000000000000000	5.919880149957742	0	0	0	0	0
	0.003091322131045	0.000107230418926	0	0	0	0	1
	0.015320591901851	0.000009556727727	1	0	0	1	0
	0.013288415642651	0.000004285244000	0	1	0	1	0
	0.012229269785063	0.000000951757181	1	0	0	1	-1
$a_2 (R_J)$	0.000000000000000	9.415417858204680	0	0	0	0	0
	0.003091322131043	0.000756924806115	0	0	0	0	1
	0.015320591903769	0.000046184290242	1	0	0	1	0
	0.012747585374909	0.000036943727087	0	0	1	1	0
	0.013288415658627	0.000023657207205	0	1	0	1	0
$a_3 (R_J)$	0.000000000000000	15.015536085998430	0	0	0	0	0
	0.003091322131051	0.000207493040720	0	0	0	0	1
	0.013288415634833	0.000035809095988	0	1	0	1	0
	0.012747585372630	0.000031633018404	0	0	1	1	0
	0.009656263252274	0.000001613346959	0	0	1	1	-1
d_1 (rad)	0.012615988896097	0.992879239808884	0	0	0	1	0
	0.009524666765044	0.084152322639125	0	0	0	1	-1
	0.015707311027184	0.084140614710325	0	0	0	1	1
	0.018798633158515	0.003627670019291	0	0	0	1	2
	0.006433344633894	0.003487460070612	0	0	0	1	-2
d_2 (rad)	0.012615988896102	0.998375521648426	0	0	0	1	0
	0.009524666765035	0.040270100082682	0	0	0	1	-1
	0.015707311027173	0.040269844497231	0	0	0	1	1
	0.018798633158461	0.000815134325314	0	0	0	1	2
	0.006433344633992	0.000808543298309	0	0	0	1	-2
z_1	-0.012615988896097	0.004190813653809	0	0	0	-1	0
	-0.009524666765039	0.000426784400617	0	0	0	-1	1
	-0.015707311027177	0.000280627379559	0	0	0	-1	-1
	0.002704603005886	0.000194145324601	1	0	0	0	0
	0.000131596475921	0.000074306914986	0	0	1	0	0
z_2	-0.012615988896101	0.009656919662512	0	0	0	-1	0
	0.000672426774343	0.000298930191083	0	1	0	0	0
	0.000131596469531	0.000254871409549	0	0	1	0	0
	-0.009524666765019	0.000213711282456	0	0	0	-1	1
	-0.015707311027141	0.000133325231924	0	0	0	-1	-1

Table 4 continued

Series	Frequency (rad/day)	Amplitude	g_1	g_2	g_3	ν_1	μ
z_3	0.000131596472831	0.001695475235159	0	0	1	0	0
	-0.012615988896102	0.000652291709819	0	0	0	-1	0
	-0.009524666765020	0.000030497500934	0	0	0	-1	1
	-0.015707311027170	0.000019535651072	0	0	0	-1	-1
	0.000672426758489	0.000011092379890	0	1	0	0	0

We analyzed the numerical series $a_j, z_j = e_j \exp i \omega_j$ and $d_j = \exp i(\lambda_j - 2\lambda_{j+1})$, obtained from numerical integrations of the averaged model. We reported only the first five terms of their quasi-periodic approximation, and we identified the corresponding frequencies as linear combinations of the fundamental frequencies $g_1, g_2, g_3, \nu_1, \mu$ (for their definition see the main text)

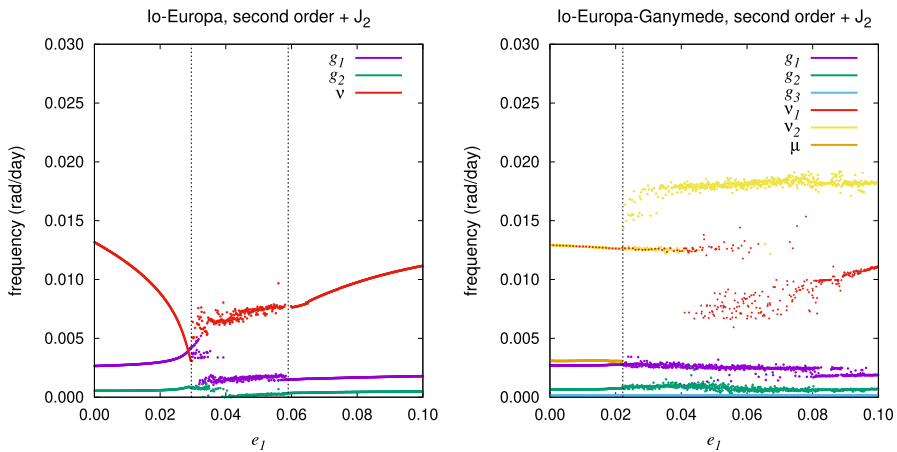


Fig. 9 Evolution of the fundamental frequencies in function of the value of e_1 for two different models. On the left, we consider the moons Io and Europa only, while, on the right, all three satellites. In both cases, the dynamical model includes first- and second-order terms in eccentricities

From $a_1 = 5.931 R_J$, we see the first signs of instability in the computation of the fundamental frequencies; even though the frequencies ν_1 and ν_2 still stick together, μ is not easily identified anymore and it disappears as we continue to increase a_1 . In the interval $(5.940, 5.952) R_J$, we observe chaos spreading further in the computation of the fundamental frequencies. This interval almost coincides with the interval occupied by the two-body MMR between Io and Europa (see Sect. 3). From the plot in Fig. 7, we can appreciate how the three-body and two-body resonant regions are well separated. The picture drawn by the fundamental frequencies shows that, with the current values of the moons’ orbital elements (especially their eccentricities), the three-body resonance permits to have a regular motion, while the two-body MMR is located in a chaotic region.

In Fig. 8, we plot the evolution of the three-body resonant angle $\lambda_1 - 3\lambda_2 + 2\lambda_3$ and Io’s eccentricity e_1 for two propagations with $a_1 = 5.92$ and $5.94 R_J$, respectively. In the first case, the bodies are well inside the three-body resonance: the angle librates with a small amplitude and the variations in eccentricity are small and show quasi-periodic features. On the contrary, in the second case, the system is inside the unstable region. We can appreciate both the chaotic path of the eccentricity and the different behaviors of the resonant angle, which

alternates phases of circulation and libration. This second evolution cannot be approximated by quasi-periodic series and indeed the computation of fundamental frequencies produces unstable values (see Fig. 7).

Finally, in Table 4, we report the frequency analysis of the system, taking $a_1 = 5.92 R_J$ and limiting the computation to the dominant five terms of the quasi-periodic series. All extracted frequencies are identified as a combination of the fundamental frequencies reported in Table 3. For easier comparison with previous works, we also performed a frequency analysis on the coordinate set of Henrard (1984), for which a further action variable is constant and the system is reduced to four degrees of freedom (see also Pucacco 2021). In that case, the four fundamental frequencies outside the three-body MMR are $\nu_1 + g_1, \nu_1 + g_2, \nu_1 + g_3$ and $\nu_1 - \nu_2$. Inside the three-body MMR, the four frequencies are $\nu_1 + g_1, \nu_1 + g_2, \nu_1 + g_3$ and μ

5 Discussion

In Sect. 4, we followed the evolution of the fundamental frequencies of the Galilean system while varying Io’s semi-major axis in a neighborhood of the resonant region. We managed to identify an interval of a_1 where the two fundamental frequencies ν_1 and ν_2 merge and the new frequency μ associated with the three-body resonance appears. In our exploration, we kept all other initial conditions unchanged. In order to map the Laplace resonance along its other dimensions, we explore also the frequencies’ response to a variation in the eccentricities.

We produce maps similar to the ones presented in Sect. 3 and 4, but this time we make Io’s mean eccentricity vary and we sample it in the interval (0, 0.1). In Fig. 9, we report the evolution of the fundamental frequencies in the case of two (left, Io–Europa) and three (right, Io–Europa–Ganymede) satellites. For both, we considered dynamical models including second-order terms in eccentricities.

In the first plot, we highlighted three intervals of e_1 (see vertical dotted lines). In the interval (0, 0.029), the motion corresponds to a circulation around the only equilibrium point of the system: the frequency ν associated with the resonant combination $\lambda_1 - 2\lambda_2$ decreases and the system approaches the resonance. In the interval (0.029, 0.059), the motion is chaotic because of the proximity to a separatrix. Finally, for $e_1 > 0.059$, the motion is regular again and it corresponds to a libration around the resonance center, so that the orbit is enclosed between the separatrices and it is far enough from them to avoid chaos.

In the second plot, we highlighted two intervals of e_1 . In the interval (0, 0.022), the bodies are inside the three-body MMR: the two frequencies ν_1 and ν_2 coincide and the three-body resonance frequency is present. Differently from the case where we made a_1 vary, the frequency μ is almost constant in this interval, so that we do not see a net decreasing due to the approaching of the three-body MMR separatrix. For $e_1 > 0.022$, the system starts to show chaotic diffusion and the two frequencies ν_1 and ν_2 become clearly separated for

Table 5 Intervals of the individual mean orbital elements in which the pure three-body MMR is identified

	a_1	a_2	a_3	e_1	e_2	e_3
Lower limit	5.911	9.406	14.952	0	0	0
Upper limit	5.930	9.422	15.052	0.022	0.029	0.078

The intervals are obtained varying only the corresponding element in the moons’ initial conditions. Semi-major axes are given in R_J units

$e_1 > 0.04$. Interestingly, for higher values of e_1 , the frequency ν_1 follows the same path presented in the left plot of Fig. 9; we deduce that Io and Europa have probably entered the two-body MMR.

Similarly to what we have shown in Sect. 3 and 4, also for e_1 we find two separated resonant intervals: one for the three-body MMR between all three moons and the other for the two-body MMR between Io and Europa. Keeping the current values of all other orbital elements, the Laplace resonance persists for small values of e_1 , while the separatrix of the two-body resonance appears for larger values of e_1 . Even though we have a clear identification of μ only for $e_1 < 0.022$, the resonance possibly occupies a larger interval ($e_1 \lesssim 0.03$), but chaos due to the proximity to the separatrix prevents fundamental frequencies to exist in this interval; in practice, the frequency analysis gives values that vary over time. The same is true also in the previous analysis for a_1 (see Sect. 4), where the region occupied by the three-body MMR is possibly slightly larger than the interval $(5.911, 5.930) R_J$. Indeed, in both cases, we can observe an intermediate region where ν_1 and ν_2 are close to each other, but their plot is quite distorted. This could be to the proximity to the separatrix of the three-body MMR. Further away, the chaos is much stronger and the frequencies are more scattered; we suspect that it is due to the appearance of the two-body MMR separatrix, and possibly to the overlap between the two-body and three-body resonances.

In Table 5, we report the ranges of all a_i and e_i ($i = 1, 3$) where the three-body resonant frequency μ is present. For computing such intervals, we made the corresponding initial condition vary, while we kept all the other unchanged. They provide a measure of the width of the Laplace resonance, which can be compared to analytical predictions present in literature (see, e.g., Pucacco 2021). Reducing the system to a pendulum-like motion, Celletti et al. (2022) computed the resonance width $\Delta\Lambda$, where Λ is the action coordinate associated with the Laplace angle. We can translate their $\Delta\Lambda$ to a width with respect to the semi-major axis Δa_i , assuming a_j fixed for $j \neq i$. By doing this, we obtain $\Delta a_1 = 0.0035$, $\Delta a_2 = 0.0165$ and $\Delta a_3 = 0.0067 R_J$. When compared with the intervals in Table 5, we find a very good agreement for the a_2 variable, while we obtain much larger widths for a_1 ($\Delta a_1 = 0.019 R_J$) and a_3 ($\Delta a_3 = 0.100 R_J$). This discrepancy is probably related to the assumptions used by Celletti et al. (2022) in order to derive their pendulum-like approximation of the Laplace resonance.

In Fig. 10, we considered all six combinations between the mean semi-major axes and eccentricities of Io and Europa, and we reported the computed value of the fundamental frequency μ , when present. As shown by the four (a_i, e_j) plots, the interval where the three-body MMR exists is larger for small eccentricities. The frequency μ decreases near the edges of the resonance due to the proximity of the separatrix. Instead, for larger eccentricities, the interval where μ can be identified becomes thinner and thinner, before it completely disappears. In the (e_1, e_2) plot, we observe that the value of μ has the smallest variation (similarly to what we already found in Fig. 9) between all six plots. We deduce that varying the eccentricities does not shift the moons with respect to the resonance center, contrary to varying their semi-major axes as one could have expected. This is particularly visible in the top right panel, where the resonance lies in a diagonal band which roughly follows the relation $n_1 - 3n_2 + 2n_3 = 0$. All plots we presented not only show that the Laplace resonance is a true three-body MMR but also that the system is very close to its center.

It is worth noting that the structure presented in the (a_2, e_2) plot of Fig. 10 is similar to the dynamical map presented by Gallardo et al. (2016) where the borders of the Laplace resonance region are numerically evaluated. The width that we can deduce from their plot coincides very well with the one we obtained (see also Table 5).

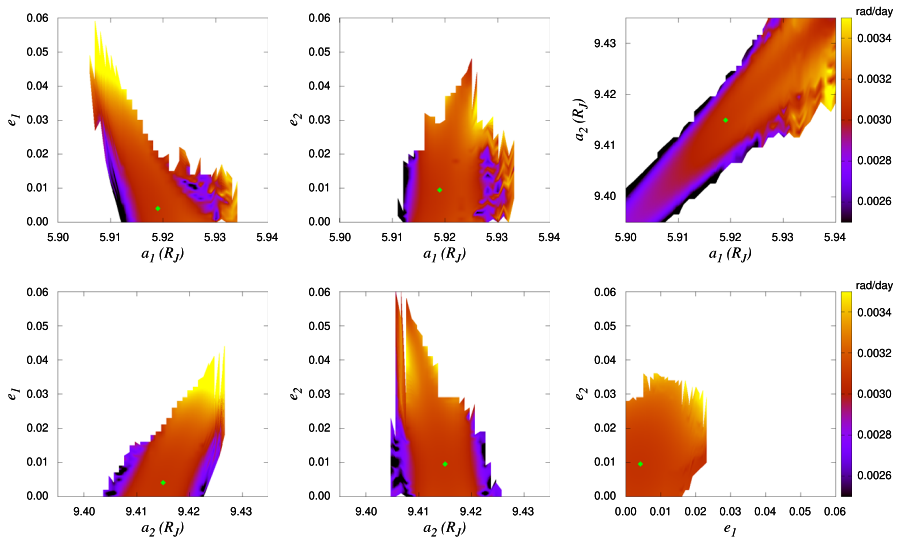


Fig. 10 Regions of the phase space where the fundamental frequency μ of the three-body resonance can be identified. For all six plots, we made two mean initial conditions vary and we performed a frequency analysis on the corresponding numerical integrations. In the white regions, the Laplace resonance is not active, while in the colored ones it is and we reported the value of the frequency μ . The green diamonds indicate the actual position of the system

Even though the above analysis focuses on the current configuration of the Galilean moons, it informs us on the pathways that may have been followed by the system in the past. The establishment of the Laplace resonance is almost certainly the result of a convergent migration of the moons, which could have happened at the time of their formation because of the drag in the circumjovian disk (Peale and Lee 2002) or on a billion-year timescale because of Jupiter's tidal dissipation (Yoder 1979). In both cases, there was one moon that migrated faster (Ganymede in the first scenario, Io in the second) and encountered the 2:1 commensurability with Europa. The two satellites then evolved maintaining the proportion in their mean motions and finally captured the last moon. If the eccentricities of the moons remained small during the evolution (for example, because of tidal dissipation), it is possible that they never entered the 2:1 MMR (i.e., the separatrix never appeared) and that the capture into the Laplace resonance of all three satellites was a smooth process. On the contrary, if the eccentricity of one or several moons has been substantial in the past, the system may have needed to cross a separatrix in order to evolve from the 2:1 MMRs to the current three-body MMR. Even though numerical simulations are essential to explore the assembly of resonant chains (see, e.g., Lari et al. 2020; Charalambous et al. 2023), an analytical study of the possible dynamical pathways would be useful in order to track down connection arcs between the two-body and three-body resonances (see, e.g., Delisle 2017). Malhotra (1991) found that the convergent evolution of the moons toward the Laplace resonance does not have a single outcome, as the moons can be trapped in other three-body MMRs. Indeed, as shown by Lari et al. (2020), before encountering the Laplace resonance ($n_1 - 3n_2 + 2n_3 \approx 0$), the system encounters the multiplet of resonances corresponding to $2n_1 - 5n_2 + 2n_3 \approx 0$ and it can be trapped by these resonances. As the moons continue to migrate outwards, the eccentricities of the two outer moons can increase up to large values ($e \approx 0.1$), before eventually this other resonant combination breaks down and the Laplace resonance is reached.

6 Conclusion

In this article, we explored the nature of the Laplace resonance between Io, Europa and Ganymede. More precisely, we wanted to investigate whether such a configuration is a pure three-body MMR or the geometric result of the superposition of two-body MMRs. To answer this, we followed the evolution of the fundamental frequencies of the system while changing the moons' initial conditions in a neighborhood of the resonant region. This way, we managed to map both the two-body and three-body MMRs.

We observed that, for some intervals of the phase space, there is a major change in the set of fundamental frequencies of the system. Indeed, far from the resonances, there are two distinct frequencies ν_1 and ν_2 , associated with the circulation of the longitude combinations $\lambda_1 - 2\lambda_2$ and $\lambda_2 - 2\lambda_3$, respectively. However, when we approach the configuration given by the Laplace relation, the two frequencies become equal, so that they cannot be defined as independent fundamental frequencies anymore. Instead, a new fundamental frequency μ appears, which is associated with the libration of the Laplace angle defined in Eq. (2). The appearance of this new fundamental frequency is the indication of the presence of a true three-body MMR. Looking at the plots in Figs. 7 and 10, we can see how the current values of the mean orbital elements of the moons place the system close to the center of this resonance. This is the result of the damping due to the tidal dissipation over hundreds millions of years after the system entered the resonance (Yoder and Peale 1981).

In contrast, by studying the dynamics of the pairs Io–Europa and Europa–Ganymede, we found that their individual two-body commensurabilities are not genuine resonances. Indeed, even though the two-body resonant angles are observed to oscillate (see Eq. 1), currently there are no separatrices associated with these resonances. Therefore, the orbits of the moons just circulate around a center that is shifted from the origin (see Fig. 3). The position of the equilibrium points is forced by the proximity to the 2:1 MMR, which is responsible for the current forced eccentricities of the satellites (Sinclair 1975).

Considering the current values of the moons' orbital elements, we found that the two-body and three-body MMRs are well separated, even though they are associated with the same ratio of the mean motions, i.e., $n_1 \approx 2n_2$ and $n_2 \approx 2n_3$. More precisely, we showed that a regular region for the Laplace resonance lies in the interval $a_1 \in (5.911, 5.930) R_J$, while the separatrix of the two-body MMR between Io and Europa appears at $a_1 \gtrsim 5.94$. Close to this limit value, chaos affects the motion because of the proximity to the separatrices. Chaotic effects are weaker closer to the three-body MMR (small scattering of the fundamental frequencies) and stronger close the two-body MMR (large scattering). The ranges of the semi-major axes given in Table 5 provide a numerical estimate of the width of the Laplace resonance which agrees in part with the analytical predictions of Celletti et al. (2022) obtained with a pendulum-like model.

For larger values of the eccentricities ($e_1 \gtrsim 0.05$), the three-body MMR disappears, while the two-body MMR is shifted toward smaller values of a_1 (see Fig. 9). Therefore, the Laplace resonance lies in the part of the phase space with moderately small eccentricities, similarly to the current configuration of the system. This is not necessarily true for other three-body MMRs, which have been observed to pump moons' eccentricities up to large values (Malhotra 1991; Showman and Malhotra 1997; Lari et al. 2020). Moreover, even different equilibrium configurations of the Laplace resonance consent larger values of the eccentricities, as observed in the exoplanetary system GJ 876 (Martí et al. 2013; Pucacco 2021).

In the end, our results show that the only true resonance of the Galilean system is the Laplace three-body MMR, which confirms what has been suggested by some previous works (Lainey et al. 2006; Gallardo et al. 2016). The other commensurabilities given by Eq. (1) are not resonances, in the sense that their related motion corresponds to a circulation instead of a proper libration. Therefore, the idea that the Galilean system consists in many simultaneous resonances, which can be found in many former (e.g., Yoder and Peale 1981; Malhotra 1991) and recent works (e.g., Lari et al. 2020; Čuk and El Moutamid 2022), is formally incorrect. However, it is possible that during the billion-year evolution of the system, two or more satellites have been trapped into genuine two-body MMRs before forming the Laplace resonance. For the future, it will be interesting to study in details the possible dynamical pathways through which the system could have passed from two-body MMRs to a three-body MMR.

Mapping fundamental frequencies can be useful also for scanning the various resonant chains observed in exoplanetary systems (Siegel and Fabrycky 2021). Charalambous et al. (2023) showed that tidal evolution of exoplanets in resonant chains makes them depart from nominal two-body MMRs and follow instead period ratios dictated by three-body MMRs. Systems with resonant chains involving more than three bodies can present more than one librating Laplace (or Laplace-like) angle (Mills et al. 2016; Leleu et al. 2021, but see also Lari et al. 2020 for the future evolution of the Galilean satellites). From their combinations, there can be oscillating angles that include the mean longitudes of four (or more) bodies. Frequency analyses of the system can reveal the presence of a libration frequencies associated with four-body commensurabilities, in order to assess whether they are the result of superposition of adjacent Laplace-like resonances or genuine four-body MMRs.

Acknowledgements The authors thank the two anonymous reviewers whose comments helped to improve and clarify this manuscript.

Author Contributions The authors contributed equally to this work.

Funding Open access funding provided by Università di Pisa within the CRUI-CARE Agreement.

Availability of data and materials All used data are available in the paper.

Code Availability All details of the code for propagating the averaged dynamical model of the Galilean satellites can be retrieved in the paper and the references therein. The code TRIP for the frequency analysis is available from the IMCCE website <https://www.imcce.fr/Equipes/ASD/trip>.

Declarations

Conflict of interest The authors declare they have no conflict of interest.

Ethical approval Not applicable.

Consent to participate Not applicable.

Consent for publication Not applicable.

Open Access This article is licensed under a Creative Commons Attribution 4.0 International License, which permits use, sharing, adaptation, distribution and reproduction in any medium or format, as long as you give appropriate credit to the original author(s) and the source, provide a link to the Creative Commons licence, and indicate if changes were made. The images or other third party material in this article are included in the article's Creative Commons licence, unless indicated otherwise in a credit line to the material. If material is not included in the article's Creative Commons licence and your intended use is not permitted by statutory

regulation or exceeds the permitted use, you will need to obtain permission directly from the copyright holder. To view a copy of this licence, visit <http://creativecommons.org/licenses/by/4.0/>.

References

- Arnold, V.I.: *Mathematical Methods of Classical Mechanics*. Springer, New York (1989)
- Batygin, K., Morbidelli, A.: Analytical treatment of planetary resonances. *Astron. Astrophys.* **556**, A28 (2013)
- Celletti, A., Karampotsiou, E., Lhotka, C., Pucacco, G., Volpi, M.: The role of tidal forces in the long-term evolution of the galilean system. *Regul. Chaotic Dyn.* **27**(4), 381–408 (2022)
- Charalambous, C., Teyssandier, J., Libert, A.-S.: Tidal interactions shape period ratios in planetary systems with three-body resonant chains. *Astron. Astrophys.* **677**, A160 (2023)
- Čuk, M., El Moutamid, M.: Three-body resonances in the saturnian system. *Astrophys. J. Lett.* **926**(2), L18 (2022)
- Delisle, J.-B.: Analytical model of multi-planetary resonant chains and constraints on migration scenarios. *Astron. Astrophys.* **605**, A96 (2017)
- Gallardo, T., Coito, L., Badano, L.: Planetary and satellite three body mean motion resonances. *Icarus* **274**, 83–98 (2016)
- Gastineau, M., Laskar, J.: Trip: a computer algebra system dedicated to celestial mechanics and perturbation series. *ACM Commun. Comput. Algebra* **44**, 194–197 (2011)
- Greenberg, R.: Orbital evolution of the Galilean satellites. In: Morrison, D. (ed.) *Satellites of Jupiter*, pp. 65–92. University of Arizona Press, Tucson (1982)
- Henrard, J.: Libration of Laplace's argument in the Galilean satellites theory. *Celest. Mech.* **34**, 255–262 (1984)
- Henrard, J., Lemaître, A.: A second fundamental model for resonance. *Celest. Mech.* **30**, 197–218 (1983)
- Lainey, V., Duriez, L., Vienne, A.: Synthetic representation of the Galilean satellites' orbital motions from 11 ephemerides. *Astron. Astrophys.* **456**(2), 783–788 (2006)
- Lari, G.: A semi-analytical model of the Galilean satellites' dynamics. *Celest. Mech. Dyn. Astron.* **130**, 50 (2018)
- Lari, G., Saillenfest, M., Fenucci, M.: Long-term evolution of the Galilean satellites: the capture of Callisto into resonance. *Astron. Astrophys.* **639**, A40 (2020)
- Lari, G., Saillenfest, M., Grassi, C.: Dynamical history of the Galilean satellites for a fast migration of Callisto. *Mon. Not. R. Astron. Soc.* **518**, 3023–3035 (2023)
- Laskar, J.: Secular evolution of the solar system over 10 million years. *Astron. Astrophys.* **198**, 341–362 (1988)
- Laskar, J.: Frequency analysis of a dynamical system. *Celest. Mech. Dyn. Astron.* **56**, 191–196 (1993)
- Leleu, A., Alibert, Y., Hara, N.C., Hooton, M.J., Wilson, T.G., Robutel, P., Delisle, J.-B., Laskar, J., Hoyer, S., Lovis, C., Bryant, E.M., Ducrot, E., Cabrera, J., Delrez, L., Acton, J.S., Adibekyan, V., Allart, R., Allende Prieto, C., Alonso, R., Alves, D., Anderson, D. R., Angerhausen, D., Anglada Escudé, G., Asquier, J., Barrado, D., Barros, S. C. C., Baumjohann, W., Bayliss, D., Beck, M., Beck, T., Bekkelien, A., Benz, W., Billot, N., Bonfanti, A., Bonfils, X., Bouchy, F., Bourrier, V., Boué, G., Brandeker, A., Broeg, C., Buder, M., Burdanov, A., Burleigh, M.R., Bérczy, T., Cameron, A.C., Chamberlain, S., Charnoz, S., Cooke, B.F., Corral Van Damme, C., Correia, A.C.M., Cristiani, S., Damasso, M., Davies, M.B., Deleuil, M., Demangeon, O.D.S., Demory, B.-O., Di Marcantonio, P., Di Persio, G., Dumusque, X., Ehrenreich, D., Erikson, A., Figueira, P., Fortier, A., Fossati, L., Fridlund, M., Futyan, D., Gandolfi, D., García Muñoz, A., García, L.J., Gill, S., Gillen, E., Gillon, M., Goad, M.R., González Hernández, J.I., Guedel, M., Günther, M.N., Haldemann, J., Henderson, B., Heng, K., Hogan, A.E., Isaak, K., Jehin, E., Jenkins, J.S., Jordán, A., Kiss, L., Kristiansen, M.H., Lam, K., Lavie, B., Lecavelier des Etangs, A., Lendl, M., Lillo-Box, J., Lo Curto, G., Magrin, D., Martins, C.J.A.P., Maxted, P.F.L., McCormac, J., Mehner, A., Micela, G., Molaro, P., Moyano, M., Murray, C.A., Nascimbeni, V., Nunes, N.J., Olofsson, G., Osborn, H.P., Oshagh, M., Ottensamer, R., Pagano, I., Pallé, E., Pedersen, P. P., Pepe, F. A., Persson, C. M., Peter, G., Piotto, G., Polenta, G., Pollacco, D., Poretti, E., Pozuelos, F.J., Queloz, D., Ragazzoni, R., Rando, N., Ratti, F., Rauer, H., Raynard, X., Rebolo, R., Reimers, C., Ribas, I., Santos, N. C., Scandariato, G., Schneider, J., Sebastian, D., Sestovic, M., Simon, A.E., Smith, A.M.S., Sousa, S.G., Sozzetti, A., Steller, M., Suárez Mascareño, A., Szabó, Gy. M., Ségransan, D., Thomas, N., Thompson, S., Tilbrook, R.H., Triaud, A., Turner, O., Udry, S., Van Grootel, V., Venus, H., Verrecchia, F., Vines, J.I., Walton, N.A., West, R.G., Wheatley, P.J., Wolter, D., Zapatero Osorio, M.R.: Six transiting planets and a chain of laplace resonances in toi-178. *Astron. Astrophys.* **649**, A26 (2021)
- Luger, R., Sestovic, M., Kruse, E., Grimm, B.-O., Demory, S.L., Agol, E., Bolmont, E., Fabrycky, D., Fernandes, C.S., Van Grootel, V., Burgasser, A., Gillon, M., Ingalls, J.G., Jehin, E., Raymond, S.N., Selsis,

- F., Triaud, A.H.M.J., Barclay, T., Barentsen, G., Howell, S.B., Delrez, L., de Wit, J., Foreman-Mackey, D., Holdsworth, D.L., Leconte, J., Lederer, S., Turbet, M., Almléaky, Y., Benkhaldoun, Z., Magain, P., Morris, B.M., Heng, K., Queloz, D.: A seven-planet resonant chain in trappist-1. *Nat. Astron.* **1**(6), 0129 (2017)
- Malhotra, R.: Tidal origin of the Laplace resonance and the resurfacing of Ganymede. *Icarus* **94**, 399–412 (1991)
- Martí, J.G., Giuppone, C.A., Beaugé, C.: Dynamical analysis of the gliese-876 laplace resonance. *Mon. Not. R. Astron. Soc.* **433**(2), 928–934 (2013)
- Michtchenko, T.A., Beaugé, C., Ferraz-Mello, S.: Dynamic portrait of the planetary 2/1 mean-motion resonance - I. systems with a more massive outer planet. *Mon. Not. R. Astron. Soc.* **387**(2), 747–758 (2008)
- Mills, S.M., Fabrycky, D.C., Migaszewski, C., Ford, E.B., Petigura, E., Isaacson, H.: A resonant chain of four transiting, sub-neptune planets. *Nature* **533**(7604), 509–512 (2016)
- Murray, C.D., Dermott, S.F.: *Solar System Dynamics*. Cambridge University Press, Cambridge (2000)
- Nesvorný, D., Morbidelli, A.: An analytic model of three-body mean motion resonances. *Celest. Mech. Dyn. Astron.* **71**(4), 243–271 (1998)
- Peale, S.J., Lee, M.H.: A primordial origin of the Laplace relation among the Galilean satellites. *Science* **298**, 593–597 (2002)
- Petit, A.C.: An integrable model for first-order three-planet mean motion resonances. *Celest. Mech. Dyn. Astron.* **133**(8), 39 (2021)
- Pucacco, G.: Normal forms for the Laplace resonance. *Celest. Mech. Dyn. Astron.* **133**(3), 11 (2021)
- Quillen, A.C.: Three-body resonance overlap in closely spaced multiple-planet systems. *Mon. Not. R. Astron. Soc.* **418**(2), 1043–1054 (2011)
- Quillen, A.C., French, R.S.: Resonant chains and three-body resonances in the closely packed inner Uranian satellite system. *Mon. Not. R. Astron. Soc.* **445**(4), 3959–3986 (2014)
- Showman, A.P., Malhotra, R.: Tidal evolution into the Laplace resonance and the resurfacing of Ganymede. *Icarus* **127**, 93–111 (1997)
- Siegel, J.C., Fabrycky, D.: Resonant chains of exoplanets: libration centers for three-body angles. *Astron. J.* **161**(6), 290 (2021)
- Sinclair, A.T.: The orbital resonance amongst the Galilean satellites of Jupiter. *Celest. Mech.* **12**, 89–96 (1975)
- Tittemore, W.C.: Chaotic motion of Europa and Ganymede and the Ganymede-Callisto dichotomy. *Science* **250**, 263–267 (1990)
- Yoder, C.F.: How tidal heating in Io drives the Galilean orbital resonance locks. *Nature* **279**, 767–770 (1979)
- Yoder, C.F., Peale, S.J.: The tides of Io. *Icarus* **47**, 1–35 (1981)

Publisher's Note Springer Nature remains neutral with regard to jurisdictional claims in published maps and institutional affiliations.